

# The complex angular-momentum plane

## 2.1 Introduction

The new idea which Regge (1959, 1960) introduced into scattering theory was the importance of analytically continuing scattering amplitudes in the complex angular-momentum plane.

At first sight this seems rather a pointless procedure because in quantum mechanics the angular momentum of a system is restricted to integer multiples of  $\hbar$  (or half-integer multiples if the particles have intrinsic spin). However, this quantization results mainly from the 'kinematics' of the process, from the invariance of the system under spatial rotations, and has little to do with the forces which determine the nature of the interaction. Thus in solving non-relativistic potential scattering problems one frequently begins by separating the Schrodinger equation into its angular and radial parts, so that one can concentrate on the radial equation (see section 3.3 below)

$$\frac{d^2\phi_l(r)}{dr^2} + \left( k^2 - \frac{l(l+1)}{r^2} - U(r) \right) \phi_l(r) = 0 \quad (2.1.1)$$

which contains the potential, and hence the dynamics of the interaction. The angular-momentum quantum number,  $l$ , appears simply as a parameter of this equation.

Normally, one would solve (2.1.1) only for the physically meaningful integer  $l$  values ( $\geq 0$ ), but there is nothing to prevent us from considering unphysical, non-integer or indeed non-real values of  $l$ . We shall see why this is of some utility in potential scattering in the next chapter, but the basic ideas are much more general than potential scattering, and are in fact more useful in elementary-particle physics.

We begin this chapter by defining partial-wave amplitudes, and discuss some of their properties, and we then consider their continuation to complex values of angular momentum. We show that the singularities which occur in the angular-momentum plane are related to the asymptotic behaviour of the scattering amplitude, and so determine the subtractions needed in dispersion relations. It is found

that moving poles in the angular-momentum plane give rise to composite particles (or resonances), so that the asymptotic behaviour of a scattering amplitude is determined by the particles which can be exchanged. This is one of the main tests of the applicability of Regge's ideas to particle physics, and provides the main topic for the rest of the book. It has also led to the introduction of the 'bootstrap hypothesis', that all strongly interacting particles may arise as a consequence of just analyticity and unitarity requirements.

## 2.2 Partial-wave amplitudes

In this chapter we shall only be concerned with  $2 \rightarrow 2$  scattering, and will restrict ourselves to spinless particles, so that the total angular momentum of the initial state is just the relative orbital angular momentum of the two particles. Since angular momentum is a conserved quantity the orbital angular momentum of the final state must be the same as that of the initial state, so it is frequently convenient to consider the scattering amplitude for each individual angular-momentum state separately, i.e. the so-called 'partial-wave' amplitudes. However, the initial state will not in general be an eigenstate of angular momentum, but a sum over many possible angular-momentum eigenstates, and hence the total scattering amplitude will be a sum over all these partial-wave amplitudes.

For spinless particles the angular dependence of the wave function describing a state of orbital angular momentum  $l$  in the  $s$  channel is given by the Legendre function of the first kind  $P_l(z_s)$  (see (A.3)). We work in the centre-of-mass system in which  $z_s \equiv \cos \theta_s$  is given by (1.7.17), so at fixed  $s$  the scattering angle is just given by  $t$  (or  $u$  from (1.7.21)), so  $t = t(z_s, s)$ .

The centre-of-mass partial-wave scattering amplitude of angular momentum  $l$  in the  $s$  channel is defined from the total scattering amplitude by

$$A_l(s) = \frac{1}{16\pi} \frac{1}{2} \int_{-1}^1 dz_s P_l(z_s) A(s, t(z_s, s)), \quad l = 0, 1, 2, \dots \quad (2.2.1)$$

The factor  $(16\pi)^{-1}$  is purely a matter of convention and is included in order to simplify the unitarity equation (2.2.7) below. We can use the orthogonality relation (A.20) to invert (2.2.1) giving

$$A(s, t) = 16\pi \sum_{l=0}^{\infty} (2l+1) A_l(s) P_l(z_s) \quad (2.2.2)$$

which is called the 'partial-wave series' for  $A(s, t)$ .

A great advantage of (2.2.2) is that at low values of  $s$  we expect only a few partial waves to contribute to the series because classically a particle with angular momentum  $l > q_s R$  (where  $q_s$  is its momentum and  $R$  is the range of the force) would miss the target and so not be scattered. Thus, very approximately, with strong interactions of range about 1 fm, only S waves should be needed for  $q_s \lesssim 200$  MeV/c, S, P waves for  $q_s \lesssim 400$  MeV/c, and so on.

Another advantage is that each partial wave satisfies its own unitarity equation independent of the others. This can be deduced by substituting the partial-wave series (2.2.2) into the two-particle unitarity relation (1.5.7) to obtain

$$16\pi \sum_l (2l+1) (A_l^{if}(s_+) - A_l^{if}(s_-)) P_l(z_s) = \frac{iq_{sn}}{16\pi^2 \sqrt{s}} (16\pi)^2 \\ \times \int_0^{2\pi} d\phi \int_{-1}^1 dz' \sum_{l'} (2l'+1) A_{l'}^{in}(s_+) P_{l'}(z') \sum_{l''} (2l''+1) A_{l''}^{nf}(s_-) P_{l''}(z'') \quad (2.2.3)$$

where  $z' \equiv \cos \theta_{in}$  is the cosine of the angle between the direction of motion of the particles in the initial state  $i$  and intermediate state  $n$ , and  $z'' \equiv \cos \theta_{nf}$  is the corresponding angle between the intermediate and final states, and of course  $z_s = \cos \theta_{if}$  (see fig. 2.1). The addition theorem of cosines gives

$$\cos \theta_{in} = \cos \theta_{if} \cos \theta_{fn} + \sin \theta_{if} \sin \theta_{fn} \cos \phi \quad (2.2.4)$$

where  $\phi$  is the angle between the scattering planes of the processes  $i \rightarrow n$  and  $n \rightarrow f$ . The addition theorem for Legendre functions (Erdelyi *et al.* (1958) p. 168) is

$$P_l(z'') = P_l(z_s) P_l(z') + 2 \sum_{m=1}^l (-1)^m \frac{\Gamma(l-m+1)}{\Gamma(l+m+1)} P_l^m(z_s) P_l^m(z') \cos m\phi \quad (2.2.5)$$

where  $P_l^m(z)$  is the associated Legendre function of the first kind. The orthogonality relation (A.20) (using Erdelyi *et al.*, p. 171) gives

$$\int_0^{2\pi} d\phi \int_{-1}^1 dz' P_{l'}(z') P_{l''}(z'') = \delta_{l'l''} \frac{4\pi}{2l'+1} P_l(z_s) \quad (2.2.6)$$

so (2.2.3) becomes

$$A_l^{if}(s_+) - A_l^{if}(s_-) = \frac{4iq_{sn}}{\sqrt{s}} A_l^{in}(s_+) A_l^{nf}(s_-) \quad (2.2.7)$$

Thus only the given angular-momentum state  $l$  is involved in the unitarity relation. The absence of factors  $16\pi$  is due to their inclusion in (2.2.1).

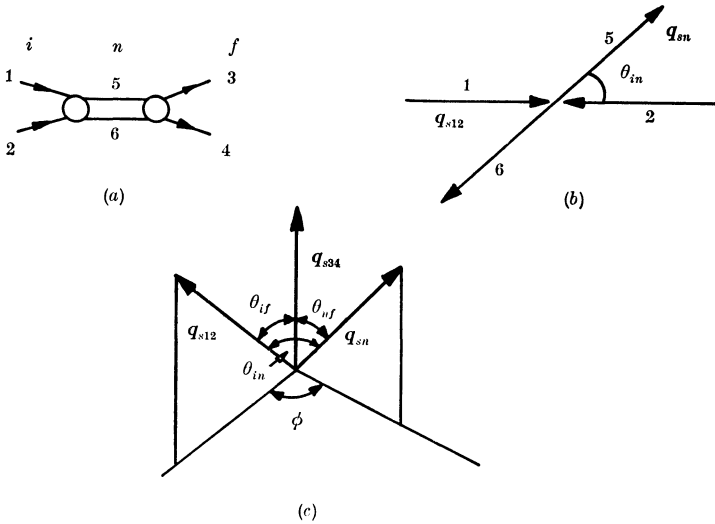


FIG. 2.1 (a) The two-body intermediate state  $|n\rangle = 5 + 6$  in  $1 + 2 \rightarrow 3 + 4$ . (b) The centre-of-mass scattering angle  $\theta_{in}$  in  $1 + 2 \rightarrow 5 + 6$ . (c) The scattering angles  $\theta_{in}$ ,  $\theta_{nI}$  and  $\theta_{nF}$ . The angle  $\phi$  is the azimuthal angle about the direction of  $\mathbf{q}_{s34}$  between the plane containing  $\mathbf{q}_{s12}$  and  $\mathbf{q}_{s34}$  and the plane containing  $\mathbf{q}_{s34}$  and  $\mathbf{q}_{sn}$ .

For elastic scattering, where the initial, intermediate and final states contain the same particles, (2.2.7) becomes, because of (1.10.3),

$$\text{Im} \{A_i^{ii}(s)\} = \frac{2q_{si}}{\sqrt{s}} |A_i^{ii}(s)|^2 = \rho^i(s) |A_i^{ii}(s)|^2 \tag{2.2.8}$$

where 
$$\rho^i(s) \equiv \frac{2q_{si}}{\sqrt{s}} \tag{2.2.9}$$

is the partial-wave phase-space factor for state  $i$ . Note that since  $\rho^i(s) \leq 1$  for all  $s$ , (2.2.8) implies that  $0 \leq \text{Im} \{A_i^{ii}\} \leq 1$ .

The relation (2.2.8) may be ensured by writing

$$A_i^{ii}(s) = \frac{e^{2i\delta_i(s)} - 1}{2i\rho^i(s)} = \frac{e^{i\delta_i(s)} \sin \delta_i(s)}{\rho^i(s)} = \frac{1}{\rho^i(s)} \frac{1}{\cot \delta_i(s) - i} \tag{2.2.10}$$

which defines the (real) ‘phase shift’  $\delta_i(s)$ . Below the inelastic threshold the scattering amplitude is completely specified by this function. By analysing the angular distribution of  $d\sigma/dt$  it is possible to determine these phase shifts directly from the experimental data, at least for the lower partial waves at small  $s$ . However, real phase shift analysis has to cope with the problems of spin (see chapter 4) and inelasticity, and is rather more difficult.

If many channels are open (2.2.7) gives

$$\begin{aligned} \text{Im} \{A_l^{ii}(s)\} &= \rho^i |A_l^{ii}(s)|^2 + \sum_{n \neq i} \rho^n A^{in}(s_+) A^{ni}(s_-) \\ &\quad + (3\text{- and more-body channels}) \end{aligned} \quad (2.2.11)$$

so 
$$0 \leq |A_l^{ii}|^2 \leq \text{Im} \{A_l^{ii}\} \leq 1 \quad (2.2.12)$$

The effect of these inelastic channels may be incorporated in (2.2.10) by allowing  $\delta_l$  to be complex,  $\delta_l \rightarrow \delta_l^R + i\delta_l^I$  so

$$A_l^{ii}(s) = \frac{\eta_l \exp(2i\delta_l^R) - 1}{2i\rho^i(s)}, \quad \text{where } \eta_l \equiv \exp(-2\delta_l^I) \quad (2.2.13)$$

$\eta_l$  being the inelasticity factor,  $0 \leq \eta_l \leq 1$ . Clearly,  $\eta_l = 1$  for elastic scattering.

If a resonance occurs in a particular partial wave at  $s = M_r^2$  (see for example Blatt and Weisskopf (1952) p. 398), then

$$\delta_l^R(s) \xrightarrow{s \rightarrow M_r^2} (2n + 1) \frac{\pi}{2} \quad (n = \text{integer})$$

so if we put say 
$$\tan \delta_l(s) \approx \frac{M_r \Gamma}{M_r^2 - s}, \quad s \approx M_r^2$$

in (2.2.10) we find

$$A_l^{ii}(s) \simeq \frac{1}{\rho^i(s)} \frac{M_r \Gamma}{M_r^2 - s - iM_r \Gamma} \simeq \frac{1}{\rho^i(s)} \frac{\Gamma/2}{M_r - E - i\Gamma/2}, \quad \text{where } E \equiv \sqrt{s} \quad (2.2.14)$$

which is the elastic Breit–Wigner resonance formula of nuclear physics, and corresponds to a resonance of mass  $M_r$  and width  $\Gamma$ . In potential scattering the condition  $\delta_l \rightarrow (2n + 1)\pi/2$  is very similar to the condition for the formation of a bound state except that a resonance occurs for positive energy and so can decay (see for example Schiff (1968) p. 128). We can thus regard resonances as unstable composite particles similar to bound states. If there is inelasticity the resonance may decay into one of several channels  $f$ , the decay amplitude being

$$A_l^{if}(s) = \frac{1}{\rho_{if}} \frac{M_r(\Gamma_i \Gamma_f)^{\frac{1}{2}}}{M_r^2 - s - iM_r \Gamma}, \quad \rho_{if} = \left(\frac{2q_i q_f}{s}\right)^{\frac{1}{2}} \quad (2.2.15)$$

where  $\Gamma_f$  is the partial width for decay into channel  $f$ , and  $\Gamma \equiv \sum_f \Gamma_f$  is the total decay width. Note the factorization of the residue of the pole. Many such resonances have been discovered in partial-wave analyses (see for example Pilkuhn (1967)).

Since  $P_l(z = 1) = 1$  for all  $l$ , the optical theorem (1.9.5) with (2.2.2) reads

$$\sigma_{12}^{\text{tot}}(s) = \frac{8\pi}{q_{s12}\sqrt{s}} \sum_l (2l + 1) \text{Im} \{A_l^{ii}(s)\} \tag{2.2.16}$$

while from (2.2.2) substituted in (1.8.13), after performing the angular integration using (A.20), we have for  $1 + 2 \rightarrow 1 + 2$

$$\sigma_{12}^{\text{el}}(s) = \frac{16\pi}{s} \sum_l (2l + 1) |A_l^{ii}(s)|^2 \tag{2.2.17}$$

Then from (2.2.8) we see that below the inelastic threshold  $\sigma_{12}^{\text{tot}} = \sigma_{12}^{\text{el}}$  as of course it must.

We can obviously make an exactly similar partial-wave decomposition in the  $t$  channel, defining

$$A_l(t) = \frac{1}{16\pi} \frac{1}{2} \int_{-1}^1 dz_t P_l(z_t) A(s(z_t, t), t), \quad l = 0, 1, 2, \dots \tag{2.2.18}$$

with inverse 
$$A(s, t) = 16\pi \sum_{l=0}^{\infty} (2l + 1) A_l(t) P_l(z_t) \tag{2.2.19}$$

In the next section we shall be concerned with the relation between (2.2.19) and scattering in the crossed  $s$  channel.

### 2.3 The Froissart–Gribov projection

Equation (2.2.19) provides a representation of the scattering amplitude which is satisfactory throughout the  $t$ -channel physical region. Since  $A_l(t)$  contains the  $t$ -channel thresholds and resonance poles the amplitude obtained from (2.2.19) has all the  $t$  singularities. But its  $s$  dependence is completely contained in the Legendre polynomials which are entire functions of  $z_t$ , and hence of  $s$  at fixed  $t$ . It is therefore evident that this representation must break down if we continue it beyond the  $t$ -channel physical region ( $-1 \leq z_t \leq 1$ ) to the nearest singularity in  $s$  (or  $u$ ) at  $s = s_0$  say, where the series will diverge. For example the pole

$$(m^2 - s)^{-1} = m^{-2} \left( 1 + \frac{s}{m^2} + \left( \frac{s}{m^2} \right)^2 + \dots \right)$$

can be represented as a polynomial in  $s$  which diverges at  $s = m^2$ .

In fig. 2.2 we have plotted the nearest  $s$ - and  $u$ -channel poles and branch points in terms of the variable  $z_t$ . They always occur outside the physical region of the  $t$  channel, but it is clear from fig. 1.5 that the use of (2.2.19) is restricted to only a small region of the Mandelstam

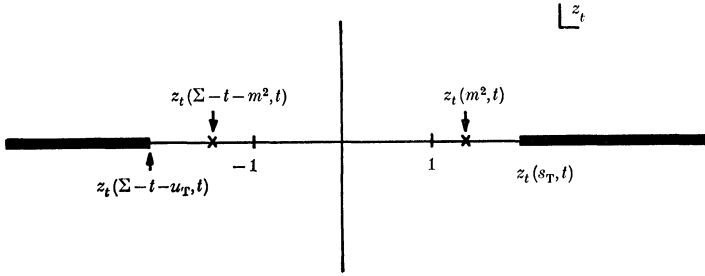


FIG. 2.2 The singularities in  $z_t$  at fixed  $t$  ( $> t_T$ ). Outside the physical region ( $-1 \leq z_t \leq 1$ ) these are the  $s$ -channel poles and threshold branch points for  $z_t > 1$ , and the  $u$ -channel singularities for  $z_t < -1$ , cf. fig. 1.5.

plot beyond the physical region. This greatly impedes the use of the crossing relation. For example, if the low- $t$  region is dominated by a resonance pole of spin  $\sigma$  it may be a good approximation to put

$$A(s, t) \approx 16\pi(2\sigma + 1) \frac{M_T \Gamma}{M_T^2 - t - iM_T \Gamma} P_\sigma(z_t) \tag{2.3.1}$$

(cf. (2.4.14) with  $\rho^i(s) \rightarrow 1$ ). However, though this may be satisfactory in the  $t$ -channel physical region, we cannot make use of it in the  $s$ -channel region ( $t \leq 0$ ) because we know that the series (2.2.19), to which (2.3.1) is an approximation, will have diverged before we can reach the  $s$  channel (see fig. 1.5).

To obtain an expression for the partial-wave amplitudes which incorporates the  $s$  and  $u$  singularities, and hence is valid over the whole Mandelstam plane, we make use of the dispersion relation (1.10.7). Since from (1.7.19), (1.7.21)

$$\left. \begin{aligned} s' - s &= 2q_{t13}q_{t24}(z'_t - z_t) \\ u' - u &= -2q_{t13}q_{t24}(z'_t - z_t) \end{aligned} \right\} \tag{2.3.2}$$

we can rewrite (1.10.7) as

$$\begin{aligned} A(s, t) &= \frac{g_s(t)}{2q_{t13}q_{t24}(z_t(m^2, t) - z_t(s, t))} \\ &\quad - \frac{g_u(t)}{2q_{t13}q_{t24}(z_t(\Sigma - t - m^2, t) - z_t(\Sigma - t - s, t))} \\ &\quad + \frac{1}{\pi} \int_{z_t(s_T, t)}^\infty \frac{D_s(s', t)}{z'_t - z_t} dz' + \frac{1}{\pi} \int_{z_t(s_T, t)}^\infty \frac{D_u(u', t)}{z'_t - z_t} dz' \end{aligned} \tag{2.3.3}$$

but subtractions may be needed in the integrals. If (2.3.3) is substituted in (2.2.18) we can perform the  $z_t$  integration using Neumann's

relation (A.14) provided the order of the two integrations can be interchanged, and we find

$$\begin{aligned}
 A_l(t) = & \frac{1}{16\pi} \frac{g_s(t)}{2q_{t13}q_{t24}} Q_l(z_t(m^2, t)) + \frac{1}{16\pi} \frac{g_u(t)}{2q_{t13}q_{t24}} Q_l(z_t(\Sigma - t - m^2, t)) \\
 & + \frac{1}{16\pi^2} \int_{z_l(s_T, t)}^\infty D_s(s', t) Q_l(z'_i) dz'_i \\
 & + \frac{1}{16\pi^2} \int_{z_l(u_T, t)}^\infty D_u(u', t) Q_l(z'_i) dz'_i, \quad l = 0, 1, 2, \dots \quad (2.3.4)
 \end{aligned}$$

This is called the Froissart-Gribov projection (Froissart 1961, Gribov 1961), and is completely equivalent to (2.2.18) provided the dispersion relation is valid. Note, however, that (2.3.4) and (2.2.18) involve completely different regions of  $z_t$  and hence  $s$ . Since (2.2.18) requires integration only over a finite region the partial-wave amplitudes can always be so defined, at least in the  $t$ -channel physical region, but (2.3.4) involves an infinite integration and can be used only if the integral converges (so that the order of the integrations can be inverted). From (A.27)  $Q_l(z) \sim z^{-l-1}$ , so if  $D_s$  (or  $D_u$ )  $\sim z^N$ , (2.3.4) is defined only for  $l > N$ . To find the lower partial waves we also need to know the subtraction functions like (1.10.10).

### 2.4 The Froissart bound

Froissart (1961) showed that, for amplitudes which satisfy the Mandelstam representation,  $s$ -channel unitarity limits the asymptotic behaviour of the scattering amplitude in the  $s$ -channel physical region,  $t \leq 0$ , and hence limits the number of subtractions which may be needed. This bound may be obtained as follows.

Since 
$$Q_l(z) \underset{l \rightarrow \infty}{\sim} l^{-\frac{1}{2}} e^{-(l+\frac{1}{2})\zeta(z)}, \quad \zeta(z) \equiv \log [z + \sqrt{z^2 - 1}] \quad (2.4.1)$$

(see (A.31)) the Froissart-Gribov projection (2.3.4) for  $s$ -channel partial waves gives

$$A_l(s) \underset{l, s \rightarrow \infty}{\longrightarrow} f(s) e^{-l\zeta(z_0)} \quad (2.4.2)$$

where  $z_0$  is the lowest  $t$ -singularity of  $A(s, t)$  (threshold or bound-state pole) and  $f(s)$  is some function of  $s$ . This means that all the partial waves with

$$l \geq l_M \equiv \zeta^{-1}(z_0) \quad (2.4.3)$$

will be very small. Indeed one may define the range of the force  $R$  (see section 2.2) that such

$$Rq_s \equiv l_M \quad (2.4.4)$$



and particles passing the target at impact parameters  $b > R$  effectively miss the target and are not scattered much. Thus for nucleon–nucleon scattering, since the pion pole is the nearest  $t$ -singularity we have (cf. (1.7.22) with  $t = m_\pi^2$ )

$$z_0 = 1 + \frac{m_\pi^2}{2q_s^2}, \quad R = \frac{1}{q_s \zeta(z_0)} \xrightarrow{s \rightarrow \infty} \frac{1}{m_\pi} = \frac{\hbar}{m_\pi c} \tag{2.4.5}$$

in our units, so the range of the force, and hence the effective size of the nucleon is 1 pion Compton wavelength, as is expected from the uncertainty principle.

Hence from (2.4.2)

$$A_l(s) \xrightarrow{l, s \rightarrow \infty} f(s) \exp(-l/Rq_s) \rightarrow \exp\left(-\frac{2l}{R\sqrt{s}} + \log f(s)\right) \tag{2.4.6}$$

since  $q_s \rightarrow \frac{1}{2}\sqrt{s}$ , and so for large  $s$  we can expect that there will only be appreciable scattering in partial waves such that

$$l < (\sqrt{s}) R \log(f(s)) \rightarrow c(\sqrt{s}) \log s \tag{2.4.7}$$

where  $c$  is some constant. Thus the partial-wave series (2.2.2) may be truncated as

$$A(s, t) \approx 16\pi \sum_{l=0}^{c(\sqrt{s}) \log s} (2l+1) A_l(s) P_l(z_s) \tag{2.4.8}$$

Then using the bound (2.2.12) and  $|P_l(z)| \leq 1$  for  $-1 \leq z \leq 1$  we have

$$|A(s, t)| \leq 16\pi \sum_{l=0}^{c(\sqrt{s}) \log s} (2l+1) \leq \text{const. } s \log^2 s, \quad s \rightarrow \infty, \quad t \leq 0 \tag{2.4.9}$$

on summing the arithmetic progression. With the optical theorem (1.9.5) this gives

$$\sigma^{\text{tot}}(s) \leq \text{const. } \log^2 s \tag{2.4.10}$$

which is the Froissart bound. It has since been proved more rigorously from field theory by Martin (1963, 1965).

For us (2.4.9) has the very important consequence that, for fixed  $t \leq 0$ ,  $D_s(s, t)$ ,  $D_u(u, t) \leq \text{const. } s \log^2 s$ ,  $s \rightarrow \infty$  so that  $N \leq 1$ , and the Froissart–Gribov projection (2.3.4) is defined for all  $l > 1$ .

Equation (2.4.6) also allows us to determine more precisely the region within which the partial-wave series (2.2.2) will converge. The asymptotic behaviour of  $P_l(z)$  is given by (A.29), which with (2.4.6) shows that (2.2.2) will converge if

$$|\text{Im}\{\theta\}| \leq \zeta(z_0) = \cosh^{-1}(z_0) \tag{2.4.11}$$

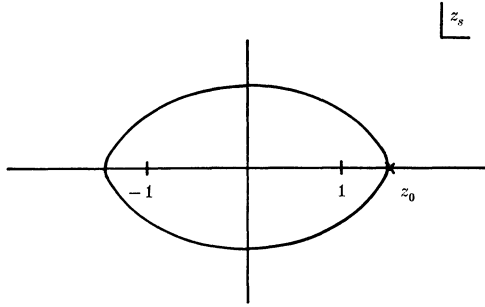


FIG. 2.3 The Lehman–Martin ellipse; the boundary of convergence of the  $s$ -channel partial-wave series in the complex  $z_s$  plane, caused by the nearest singularity at  $z_s = z_0$ .

which defines an ellipse in the complex  $z_s$  plane with foci at  $z_s = \pm 1$  and semi-major axis  $z_0$  (see fig. 2.3). This is often referred to as the small Lehmann–Martin ellipse (Lehmann 1958, Martin 1966).

2.5 Signature

In (2.3.4)  $A_l(t)$  is defined in terms of integrals over the right-hand ( $s$ -channel) and left-hand ( $u$ -channel) cuts in  $z_t$  (fig. 2.2). The asymptotic behaviour of these contributions as  $l \rightarrow \infty$  is readily obtained from (2.4.2). On the right-hand cut  $z_t$  is always  $> 1$  so  $\zeta(z)$  is always real and positive, for  $t > t_T$ , so

$$A_l^{RH} \xrightarrow{l \rightarrow \infty} f(t) e^{-l\zeta(z_0)}, \quad z_0 \equiv z_t(s_0, t) \tag{2.5.1}$$

However, along the left-hand cut  $z_t < -1$  so

$$\zeta(z) = \zeta(|z|) + i\pi \quad \text{and} \quad A_l^{LH} \xrightarrow{l \rightarrow \infty} f(t) e^{-l\zeta(|z_0|)} e^{-i\pi l} \tag{2.5.2}$$

which is unbounded as  $l \rightarrow i\infty$ . In section 2.7 we shall want to express the scattering amplitude as a contour integral in the complex  $l$  plane, but we should be hindered by such a divergent behaviour.

Instead, therefore, we define partial-wave amplitudes of definite signature  $\mathcal{S} = \pm 1$  by (neglecting the pole terms for simplicity)

$$\begin{aligned} A_l^{\mathcal{S}}(t) &= \frac{1}{16\pi^2} \int_{z_T}^{\infty} D_s(s', t) Q_l(z'_i) dz'_i + \mathcal{S} \frac{1}{16\pi^2} \int_{z_T}^{\infty} D_u(s', t) Q_l(z'_i) dz'_i \\ &= \frac{1}{16\pi^2} \int_{z_T}^{\infty} (D_s(s', t) + \mathcal{S} D_u(s', t)) Q_l(z'_i) dz'_i \\ &\equiv \frac{1}{16\pi^2} \int_{z_T}^{\infty} D_s^{\mathcal{S}}(s', t) Q_l(z'_i) dz'_i \end{aligned} \tag{2.5.3}$$

where  $D_s^{\mathcal{S}}(s, t) \equiv D_s(s, t) + \mathcal{S}D_u(s, t)$ , and where both integrals run over positive  $z_t$  (for  $t > t_T$ ). Amplitudes with  $\mathcal{S} = +1$  are referred to as having even signature, while those with  $\mathcal{S} = -1$  have odd signature. Since  $Q_l(z)$  satisfies the reflection relation (A.17) it should be clear by comparison with (2.3.4) that

$$\left. \begin{aligned} A_l^+(t) &= A_l(t) & \text{for } l = 0, 2, 4, \dots \\ A_l^-(t) &= A_l(t) & \text{for } l = 1, 3, 5, \dots \end{aligned} \right\} \quad (2.5.4)$$

These physical integer values of  $l$  are referred to as the ‘right-signature points’ of  $A_l^{\mathcal{S}}(t)$  (i.e. even  $l$  for even signature, and vice versa) and conversely the unphysical integer values (i.e. odd  $l$  for even signature, and vice versa) are called ‘wrong-signature points’. With the definition (2.5.3)

$$A_l^{\mathcal{S}}(t) \xrightarrow[l \rightarrow \infty]{} f(t) e^{-l\xi(z_0)}, \quad \text{for } \mathcal{S} = \pm 1 \quad (2.5.5)$$

and so converges as  $l \rightarrow \infty$ .

We can sum the partial-wave series to give amplitudes of definite signature

$$A^{\mathcal{S}}(s, t) \equiv 16\pi \sum_{l=0}^{\infty} (2l+1) A_l^{\mathcal{S}}(t) P_l(z_t) \quad (2.5.6)$$

so the even part of  $A^+(s, t)$  in  $z_t = \text{even part of } A(s, t)$ , and the odd part of  $A^-(s, t) = \text{odd part of } A(s, t)$ . These amplitudes satisfy the dispersion relation (again omitting poles)

$$A^{\mathcal{S}}(s, t) = \frac{1}{\pi} \int_{s_T}^{\infty} \frac{D_s(s', t)}{s' - s} ds' + \mathcal{S} \frac{1}{\pi} \int_{u_T}^{\infty} \frac{D_u(u', t)}{u' - s} du' \quad (2.5.7)$$

$$= \frac{1}{\pi} \int_{s_T}^{\infty} \frac{D_s^{\mathcal{S}}(s', t)}{s' - s} ds' \quad (2.5.8)$$

where  $s$  has replaced  $u$  in the denominator of the second term because of the replacement  $z_t \rightarrow -z_t$  in the corresponding term of (2.5.3). The Mandelstam representation for such an amplitude is from (1.11.4), (1.11.5) in (2.5.7) (with some changes of variables)

$$\begin{aligned} A^{\mathcal{S}}(s, t) &= \frac{1}{\pi^2} \iint^{\infty} \frac{\rho_{st}(s, t'') + \mathcal{S}\rho_{tu}(s', t'')}{(s' - s)(t'' - t)} ds' dt'' \\ &\quad + \frac{1}{\pi^2} \iint^{\infty} \frac{\rho_{su}(s', t'') + \mathcal{S}\rho_{su}(u'', s')}{(s' - s)(u'' - u')} ds' du'' \end{aligned} \quad (2.5.9)$$

The lack of symmetry in  $s, t$  and  $u$  stems from the fact that we have taken definite signature in the  $t$  channel. These definite-signature

amplitudes are of course unphysical because of the change of the sign of  $z_t$  involved in the definition (2.5.3). But from (2.5.6) with (2.5.4) and (A.11) it is possible to obtain the physical amplitude from them by

$$A(s, t) = \frac{1}{2}(A^+(z_t, t) + A^+(-z_t, t) + A^-(z_t, t) - A^-(-z_t, t)) \quad (2.5.10)$$

For analytic continuation in  $l$  we shall always use  $A^{\mathcal{S}}(s, t)$  rather than  $A(s, t)$ .

Since with equal-mass kinematics  $z_t$  is given by (1.7.22), it has a pole at  $t = t_T \equiv 4m^2$ . So, from (2.5.1), for  $t < t_T$  it is

$$\hat{A}_l^{\mathcal{S}}(t) \equiv e^{inl} A_l^{\mathcal{S}}(t) \quad (2.5.11)$$

which has the good asymptotic  $l$  behaviour, rather than  $A_l^{\mathcal{S}}(t)$  itself. But we shall find in the next section that the threshold behaviour is  $A_l^{\mathcal{S}}(t) \sim (q_t^2)^l \sim (t - 4m^2)^l$  so the required factor (2.5.11) is included automatically.

## 2.6 Singularities of partial-wave amplitudes and dispersion relations\*

In the  $t$ -channel physical region we can obtain the signed partial-wave amplitudes either from (2.2.18) and (2.5.6), i.e.

$$A_l^{\mathcal{S}}(t) = \frac{1}{32\pi} \int_{-1}^1 A^{\mathcal{S}}(s, t) P_l(z_t) dz_t, \quad l = 0, 1, 2, \dots \quad (2.6.1)$$

or equivalently from (2.5.3) and (2.5.8), i.e.

$$A_l^{\mathcal{S}}(t) = \frac{1}{16\pi^2} \int_{z_T}^{\infty} D_s^{\mathcal{S}}(s, t) Q_l(z_t) dz_t, \quad l = 0, 1, 2, \dots \quad (2.6.2)$$

Since  $2D_s^{\mathcal{S}}(s, t)$  is the discontinuity of  $A^{\mathcal{S}}(s, t)$  across the cuts in  $z_t$ , while from (A.15) the discontinuity of  $Q_l(z)$  is  $-\pi P_l(z)$ , we can combine (2.6.1) and (2.6.2) in

$$A_l^{\mathcal{S}}(t) = \frac{1}{32\pi^2} \int_{C_1 \text{ or } C_2} A^{\mathcal{S}}(s, t) Q_l(z_t) dz_t \quad (2.6.3)$$

where the contours encircle the cuts of either  $Q_l(z_t)$  or  $A^{\mathcal{S}}(s, t)$  as shown in fig. 2.4.

Since the integration in (2.6.1) is over a finite  $s$  region, at fixed  $t$ , it is clear that  $A_l^{\mathcal{S}}(t)$  will have all the  $t$ -channel threshold branch points of  $A^{\mathcal{S}}(s, t)$  which also occur at fixed  $t$ . In (2.6.2) these branch points

\* This section may be omitted at first reading.

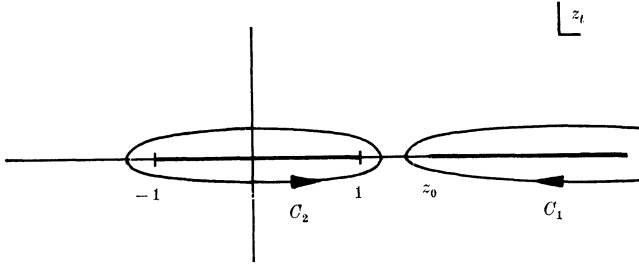


FIG. 2.4 Integration contours in the complex  $z_t$  plane used in (2.6.3).

appear in  $D_s^{\mathcal{S}}(s, t)$ . They are of course generated by the unitarity equations as discussed in chapter 1.

However, the partial-wave projection may introduce further threshold singularities. These arise from the vanishing of the three-momenta which appear in the expression for  $z_t$ , (1.7.19). Thus at the threshold for the initial state  $t \rightarrow (m_1 + m_3)^2$ ,  $\lambda(t, m_1^2, m_3^2) \rightarrow 0$ ,  $q_{t13} \rightarrow 0$ , so  $z_t \rightarrow \infty$ . In view of the asymptotic behaviour of Legendre functions (A.27),  $Q_l(z_t) \sim (z_t)^{-l-1}$ , this means

$$Q_l(z_t) dz_t \sim [t - (m_1 + m_3)^2]^{l/2} \quad (2.6.4)$$

$$\text{and so from (2.6.2)} \quad A_l^{\mathcal{S}}(t) \sim [t - (m_1 + m_3)^2]^{l/2} \quad (2.6.5)$$

Also  $q_{t13}$  vanishes at the so-called 'pseudo-threshold'  $t \rightarrow (m_1 - m_3)^2$  and  $q_{t14} \rightarrow 0$  at  $t \rightarrow (m_2 \pm m_4)^2$ , so if we introduce the notation

$$T_{ij}^{\pm}(t) \equiv [t - (m_i \pm m_j)^2]^{\frac{1}{2}} \quad (2.6.6)$$

$$\text{we find} \quad A_l^{\mathcal{S}}(t) \sim (T_{13}^+(t) T_{13}^-(t) T_{24}^+(t) T_{24}^-(t))^l \quad (2.6.7)$$

If the initial- and final-state thresholds coincide, i.e.  $m_1 + m_2 = m_3 + m_4$ , there is simply a kinematical zero of order  $l$  at the threshold, but otherwise there are square-root branch points for odd values of  $l$ . What is worse, if we want to continue to non-integer values of  $l$ , (2.6.7) implies that there will always be kinematical branch points. So if we wish to write dispersion relations for the partial-wave amplitudes, integrating over just the dynamical singularities as we did for the full amplitude in (1.10.7), we must first remove these kinematical singularities by defining the 'reduced' partial-wave amplitudes

$$B_{i_{\mu}}^{\mathcal{S}}(t) \equiv A_l^{\mathcal{S}}(t) (q_{t13} q_{t24})^{-l} \quad (2.6.8)$$

whose threshold singularities in  $t$  are just the dynamical threshold

branch points. Clearly  $B_l^{\mathcal{S}}(t)$  is Hermitian analytic if  $A^{\mathcal{S}}(s, t)$  is (see section 1.5).

The positive  $t$ , or right-hand cut discontinuity of this amplitude may be obtained from (2.5.9) in (2.6.2) with (2.6.8), viz.

$$\text{Im} \{B_l^{\mathcal{S}}(t)\}_{\text{RH}} = \frac{1}{16\pi^2} \int_{z_0}^{\infty} (\rho_{st}(s', t) + \mathcal{S}\rho_{tu}(s', t)) Q_l(z'_t) dz'_t (q_{t13} q_{t24})^{-l} \tag{2.6.9}$$

In addition to these thresholds  $A^{\mathcal{S}}(s, t)$  may also have fixed- $t$  singularities due to bound-state poles below threshold. Thus a  $t$ -channel bound state of mass  $M$  and spin  $\sigma$  contributes

$$A^{\mathcal{S}}(s, t) = \frac{(2\sigma + 1) g_t^2 (q_{t13} q_{t24})^\sigma}{M^2 - t} P_\sigma(z_t) \tag{2.6.10}$$

where  $g_t^2$  is the coupling strength (the factor  $(2\sigma + 1)$  is purely conventional) and we have included the threshold factor  $(q_{t13} q_{t24})^\sigma$  explicitly (so that  $g_t$  may be constant). In (2.2.18) with (A.20) and (2.6.8) this gives

$$B_l^{\mathcal{S}}(t) = \frac{1}{16\pi} \frac{g_t^2}{M^2 - t} \delta_{l\sigma} \tag{2.6.11}$$

a contribution to the  $l = \sigma$  partial wave only. These right-hand singularities are exhibited in fig. 2.5 where we have drawn the threshold cuts along the positive  $t$  axis.

However, there are further singularities which occur at negative values of  $t$  due to the  $s$ -channel singularities of  $A^{\mathcal{S}}(s, t)$ . (Remember  $A^{\mathcal{S}}(s, t)$  has no  $u$  singularities as these have been folded over into the  $s$  channel by (2.5.3).) Thus suppose there is a bound-state pole in the  $s$  channel of spin  $\sigma$  and mass  $M$ ,

$$A^{\mathcal{S}}(s, t) = \frac{(2\sigma + 1) g_s^2 (q_{s12} q_{s34})^\sigma P_\sigma(z_s)}{M^2 - s} \tag{2.6.12}$$

$$\equiv \frac{G_s(s)}{M^2 - s} P_\sigma(z_s)$$

so 
$$D^{\mathcal{S}}(s, t) = \pi G_s(s) P_\sigma(z_s(s, t)) \delta(s - M^2) \tag{2.6.13}$$

which substituted in (2.5.3) gives, through (2.6.8),

$$B_l^{\mathcal{S}}(t) = G_s(M^2) P_\sigma(z_s(M^2, t)) Q_l(z_t(M^2, t)) (q_{t13} q_{t24})^{-l} \tag{2.6.14}$$

Now  $Q_l(z)$  has branch points in  $z$  at  $z = \pm 1$  (for integer  $l$ ) and so (2.6.14) has singularities at

$$z_t(M^2, t) = \pm 1$$

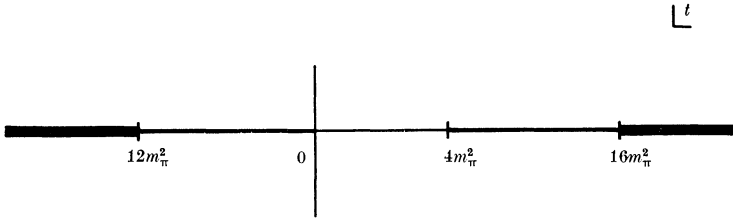


FIG. 2.5 Singularities of the  $t$ -channel partial-wave amplitudes for  $\pi\pi$  scattering, showing the thresholds at  $t = (2m_\pi)^2, (4m_\pi)^2, \dots$  and the left-hand cuts at  $t = 4m_\pi^2 - s_{\pi i}$  where  $s_{\pi i}$  are the  $s$ -channel thresholds at  $s = (2m_\pi)^2, (4m_\pi)^2, \dots$  (Note that  $G$ -parity forbids odd numbers of pions, see section 5.1.)

which from (1.7.19) requires

$$\frac{t^2 + t(2M^2 - \Sigma) + (m_1^2 - m_3^2)(m_2^2 - m_4^2)}{\lambda^{\frac{1}{2}}(t, m_1^2, m_3^2) \lambda^{\frac{1}{2}}(t, m_2^2, m_4^2)} = \pm 1 \quad (2.6.15)$$

For example if all the external particles have equal masses (e.g. for  $\pi\pi \rightarrow \pi\pi$ ,  $m_1 = m_2 = m_3 = m_4 = m_\pi$ ), this reduces to

$$1 + \frac{2M^2}{t - 4m_\pi^2} = \pm 1 \quad (2.6.16)$$

so there are branch points at  $t = \infty$  and at  $t = 4m_\pi^2 - M^2$ , and conventionally the branch cut is drawn along the negative  $t$  axis as in fig. 2.5. Note that the  $s$ -channel pole of spin  $\sigma$  contributes to all the partial waves of the  $t$  channel through (2.6.14).

The singularity arises through a pinch of the singularity of  $A^\sigma(s, t)$  with the branch points of  $Q_i(z)$  in (2.5.3). All the other  $s$ -singularities, the threshold branch points etc., will give similar pinches, and hence similar left-hand branch points, at positions determined simply by replacing  $M^2$  in (2.6.16) by the (real) threshold value of  $s$ .

For unequal-mass kinematics the mapping of the  $s$  singularities into  $t$  is much more complicated. There are four solutions to (2.6.15), two being independent of  $M^2$ , i.e.  $t = 0$  and  $\infty$ . Thus for  $\pi N$  scattering the  $N$  exchange pole generates branch points at  $t = 0, \infty, (M_N - m_\pi^2/M_N)^2$  and  $M_N^2 + 2m_\pi^2$ . (Note that if  $m_\pi \rightarrow M_N$  these two cuts join up, giving a single cut at  $t = 3M_N^2$  in agreement with (2.6.16).) (For further details see for example Martin and Spearman (1970) p. 376 *et seq.*)

Since the imaginary part of  $Q_i$  is given by (A.15) for integer  $l$ , we find from (2.5.3) that

$$\text{Im} \{A_l^\sigma(t)\}_{\text{LH}} = \frac{1}{32\pi} \int_{-1}^{z_0} P_l(z'_i) D_s^\sigma(s', t) dz'_i \quad (2.6.17)$$

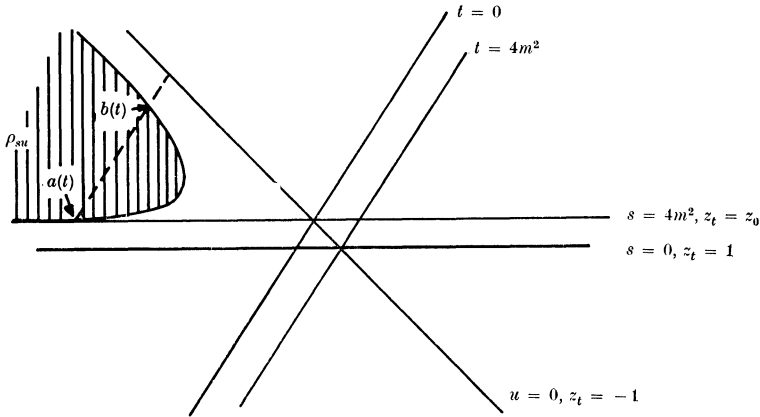


FIG. 2.6 Singularities in the Mandelstam plot involved in the partial-wave projection of a definite-signature  $t$ -channel amplitude. The left-hand cut for negative (fixed)  $t$  involves integration over the  $s$ -singularities between  $z_t = z_0$  (the nearest  $s$ -singularity) and  $z_t = -1$ . For sufficiently negative  $t$  this includes integration over the double spectral function between the boundary points  $a(t)$  and  $b(t)$  as well, the dashed line being the fixed- $t$  integration contour.

( $z_0$  being the lowest  $s$ -singularity – see fig. 2.6) gives the discontinuity of  $A_l^{\mathcal{S}}(t)$  along its left-hand cut. For non-integer  $l$  we need to use (A.16), but we are more interested in the singularities of  $B_l^{\mathcal{S}}(t)$ , and, for  $s > 0$ ,  $t \pm i\epsilon$  corresponds to  $z \pm i\epsilon$  (from (1.7.19)), so the branch point of  $Q_l(z)$  at  $z = -1$  is cancelled by that of the kinematical factor (2.6.8), i.e.  $Q_l(z_t) (q_{t13}q_{t24})^{-1}$  has no cut for  $z_t < -1$ . There is a contribution from the cut of  $Q_l(z_t)$  for  $-1 < z_t < 1$ , and another from the discontinuity of  $D_s(s, t)$  in the negative  $t$  region, obtained from (2.5.9), so

$$\begin{aligned} \text{Im} \{B_l^{\mathcal{S}}(t)\}_{\text{LH}} &= \frac{1}{32\pi} \int_{-1}^{z_0} P_l(-z'_t) D_s^{\mathcal{S}}(s', t) dz'_t (-q_{t13}q_{t24})^{-1} \\ &+ \frac{1}{16\pi^2} \int_{a(t)}^{b(t)} Q_l(z'_t) (\rho_{su}(s', u') + \mathcal{S} \rho_{su}(u', s')) dz'_t (q_{t13}q_{t24})^{-1} \end{aligned} \quad (2.6.18)$$

where the regions of integration are shown in fig. 2.6. Since interchanging  $s$  and  $u$  is equivalent to changing the sign of  $z_t$ , with (A.17) (2.6.18) becomes

$$\begin{aligned} \text{Im} \{B_l^{\mathcal{S}}(t)\}_{\text{LH}} &= \frac{1}{32\pi} \int_{-1}^{z_0} P_l(-z'_t) D_s^{\mathcal{S}}(s', t) dz'_t (-q_{t13}q_{t24})^{-1} \\ &+ \frac{1}{16\pi^2} \int_{a(t)}^{b(t)} Q_l(z'_t) \rho_{su}(s', u') (1 - \mathcal{S} e^{-i\pi l}) dz'_t (q_{t13}q_{t24})^{-1} \end{aligned} \quad (2.6.19)$$

This last term, which is due to the fact that an exchange force (and



hence the  $\rho_{su}$  double spectral function) is present, does not contribute at right-signature values of  $l$  where  $e^{-i\pi l} = \mathcal{S}$ .

With this knowledge of the singularity structure we can write down dispersion relations for the reduced partial-wave amplitudes

$$B_l^{\mathcal{S}}(t) = \frac{1}{\pi} \int_{\text{RH}} \frac{\text{Im}\{B_l^{\mathcal{S}}(t')\}}{t'-t} dt' + \frac{1}{\pi} \int_{\text{LH}} \frac{\text{Im}\{B_l^{\mathcal{S}}(t')\}}{t'-t} dt' \quad (2.6.20)$$

both discontinuities being given by the double spectral functions in (2.6.9) and (2.6.19). Particular care is needed with subtractions, however, because in taking out the threshold behaviour in (2.6.8) we have worsened the asymptotic  $t$  behaviour. Such dispersion relations are widely used in parameterizing partial waves, for example in phase-shift analyses. Of particular importance is the fact that crossing is readily incorporated because the crossed channel singularities appear in the left-hand cut. Also the right-hand cut discontinuity is given by the unitarity equation. From (2.2.7) (interchanging  $s$  and  $t$ ) with (2.6.8) we find

$$B_l^{\mathcal{S}if}(t_+) - B_l^{\mathcal{S}if}(t_-) = 2i \sum_n \rho_i^n(t) B_l^{\mathcal{S}in}(t_+) B_l^{\mathcal{S}nf}(t_-) + \text{3- and more-body intermediate states} \quad (2.6.21)$$

where 
$$\rho_i^n(t) \equiv (q_{t13} q_{t24})^n \frac{q_{tn}}{\sqrt{t}} \quad (2.6.22)$$
 and in the elastic region (cf. (2.2.8))

$$\text{Im}\{B_l^{\mathcal{S}ii}(t)\} = \frac{2(q_{t13})^{2l+1}}{\sqrt{t}} |B_l^{\mathcal{S}ii}(t)|^2 \quad (2.6.23)$$

This form of the unitarity equation will be useful for analytic continuation in  $l$ .

### 2.7 Analytic continuation in angular momentum

The Froissart–Gribov projection, (2.6.2), may be used to define  $A_l^{\mathcal{S}}(t)$  for all values of  $l$ , not necessarily integer or even real, as we have been assuming so far. In fact, it can be used for all  $l$  such that  $\text{Re}\{l\} > N(t)$ , where  $D_s$  (or  $D_u$ )  $\sim z^{N(t)}$ , and where  $N(t) \leq 1$  for  $t \leq 0$  from (2.4.9). The main advantage of using (2.6.2) rather than (2.2.18) for  $l \neq$  integer is that  $Q_l$  has a better behaviour than  $P_l$  as  $l \rightarrow \infty$  (compare (A.28) and (A.31)).

The only singularities of  $Q_l(z)$  are poles at  $l = -1, -2, \dots$  (see (A.32)), so (2.6.2) defines a function of  $l$  which is holomorphic (free of singularities) for  $\text{Re}\{l\} > \max(N(t), -1)$ .

It is not immediately apparent that there is much merit to this extended definition of the partial-wave amplitudes because of course it is only positive integer values of  $l$  that have physical significance, and there is clearly an infinite number of different ways of interpolating between the integers. However  $A_l^{\mathcal{S}}(t)$  defined by (2.6.2) vanishes as  $|l| \rightarrow \infty$  (see (2.5.5)) and a theorem due to Carlson (proved in Titchmarsh (1939) p. 186) tells us that (2.6.2) must be the unique continuation with this property.

More precisely Carlson’s theorem states that: if  $f(l)$  is regular, and of the form  $O(e^{k|l|})$ , where  $k < \pi$ , for  $\text{Re}\{l\} \geq n$ , and  $f(l) = 0$  for an infinite sequence of integers,  $l = n, n + 1, n + 2, \dots$ , then  $f(l) = 0$  identically. Thus if we were to write

$$A_l^{\mathcal{S}}(t) = A_l^{FG}(t) + f(l, t)$$

where  $A_l^{FG}(t)$  is obtained from the Froissart–Gribov projection, and  $f(l, t) = 0$  for integer  $l$ , the theorem tells us that either  $A_l^{\mathcal{S}}(t) \rightarrow 0$  as  $|l| \rightarrow \infty$  or  $f(l, t)$  vanishes everywhere. Perhaps the simplest example is

$$A_l^{\mathcal{S}}(t) = A_l^{FG}(t) + F(t) \sin \pi l$$

Remembering that  $\sin \pi l = (e^{i\pi l} - e^{-i\pi l}) (2i)^{-1}$  it is clear that  $|A_l^{\mathcal{S}}(t)| \rightarrow \infty$  as  $l \rightarrow i\infty$ , due to the added term.

Hence (2.6.2) defines  $A_l^{\mathcal{S}}(t)$  uniquely as a holomorphic function of  $l$  with convergent behaviour as  $|l| \rightarrow \infty$ , for all  $\text{Re}\{l\} > N(t)$ . However, we are prevented from continuing below  $\text{Re}\{l\} = N(t)$  by the divergent behaviour of  $D_s(s, t)$  as  $s \rightarrow \infty$ .

To proceed further we must make the additional, and crucial, assumption that the scattering amplitude  $A_l(t)$  is an analytic function of  $l$  throughout the complex angular-momentum plane, with only isolated singularities. It will then be just these isolated singularities which cause the divergence problems, and we can easily continue past them.

For example suppose that  $D_l^{\mathcal{S}}(s, t)$  has a leading asymptotic power behaviour

$$D_s^{\mathcal{S}}(s, t) \sim s^{\alpha(t)} + \text{lower order terms} \tag{2.7.1}$$

so  $N(t) = \alpha(t)$ . Then, since from (A.27)  $Q_l(z) \sim z^{-l-1}$ , and from (1.7.19)  $z_t \xrightarrow{s \rightarrow \infty} s/q_{t13} q_{t24}$ , the large- $s$  region of (2.6.2) ( $s > s_1$  say) gives

$$A_l^{\mathcal{S}}(t) \sim \int_{l > \alpha(t)}^{\infty} s^{\alpha(t)} s^{-l-1} ds = - \frac{e^{\alpha(t)-l} \log s_1}{\alpha(t) - l} \tag{2.7.2}$$

Hence  $A_l(t)$  has a pole at  $l = \alpha(t)$ . This is, by hypothesis, the rightmost

singularity in the complex  $l$  plane, and it is this singularity which is preventing continuation to the left of  $\text{Re}\{l\} = \alpha(t)$ . However, once we have isolated this pole we can continue round it to the left, until we reach the singularity due to the next term in the asymptotic expansion of  $D_s^{\mathcal{S}}(s, t)$ .

There may be logarithmic terms like

$$D_s^{\mathcal{S}}(s, t) \sim s^{\alpha(t)} (\log s)^{\beta(t)} \quad (2.7.3)$$

giving

$$\begin{aligned} A_l^{\mathcal{S}}(t) &\sim \int_{l > \alpha(t)}^{\infty} s^{\alpha(t)} (\log s)^{\beta(t)} s^{-l-1} ds = \frac{1}{(\alpha(t) - l)^{1+\beta(t)}} + \dots, \quad \beta(t) \neq -1 \\ &= \log(\alpha(t) - l), \quad \beta(t) = -1 \end{aligned} \quad (2.7.4)$$

so  $A_l^{\mathcal{S}}(t)$  has a branch point at  $l = \alpha(t)$ , or a multiple pole if  $\beta$  is a positive integer. We shall discuss the physical significance of these poles and branch points below.

The assumption that  $A_l^{\mathcal{S}}(t)$  has only isolated singularities in  $l$ , and so can be analytically continued throughout the complex angular-momentum plane, is sometimes called the postulate of 'maximal analyticity of the second kind', to distinguish it from postulate (v) of section 1.4 concerning analyticity in  $s$  and  $t$ . It is the basic assumption upon which the applicability of Regge theory to particle physics rests. It is certainly not proven, but, as we shall see in the next chapter, it is true of various plausible models for strong interactions, and, much more important, it seems to be in accord with experiment.

If it is true, then the partial-wave series (2.5.6) can be rewritten as a contour integral in the  $l$  plane (a method used by Sommerfeld (1949), following a technique of Watson (1918)), viz.

$$A^{\mathcal{S}}(s, t) = -\frac{16\pi}{2i} \int_{C_1} (2l+1) A_l^{\mathcal{S}}(t) \frac{P_l(-z_t)}{\sin \pi l} dl \quad (2.7.5)$$

The contour  $C_1$  is shown in fig. 2.7. It embraces the positive integers and zero, but avoids any singularities of  $A_l(t)$ . The residues of the poles of the integrand at the integers  $l = n$ , where  $\sin \pi l \rightarrow (-l)^n (l-n)\pi$ , are

$$\frac{2\pi i(2n+1) A_n^{\mathcal{S}}(t) P_n(-z_t)}{(-1)^n \pi} = 2i(2n+1) A_n^{\mathcal{S}}(t) P_n(z_t) \quad (2.7.6)$$

using (A.11), so Cauchy's theorem gives, from (2.7.5)

$$A_l^{\mathcal{S}}(s, t) = 16\pi \sum_l (2l+1) A_l^{\mathcal{S}}(t) P_l(z_t) \quad (2.7.7)$$

Hence (2.7.5) is equivalent to (2.7.7) provided  $A_l(t)$  has the required analyticity in  $l$ .

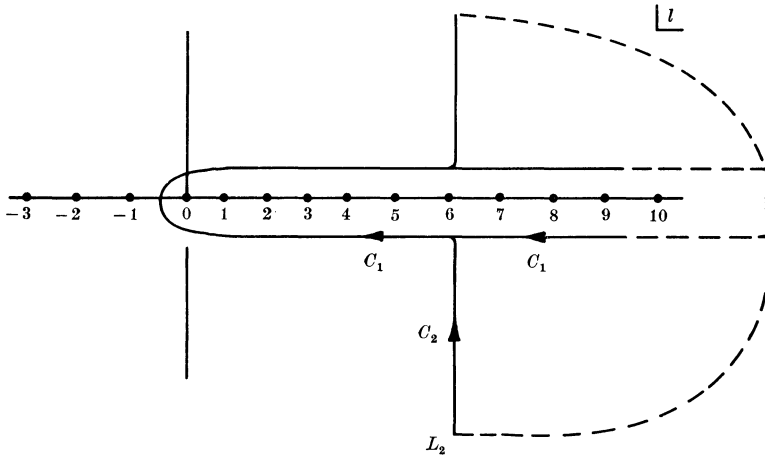


FIG. 2.7 The integration contour  $C_1$  in the complex  $l$  plane enclosing the positive integers. This is then opened up along the line  $\text{Re}\{l\} = L_2$  to give the contour  $C_2$  with a semi-circle at infinity.

Since we have found that  $A_l^{\mathcal{S}}(t)$  has no singularities in  $\text{Re}\{l\} > N(t)$  we can displace the contour from  $C_1$  to  $C_2$ , shown in fig. 2.7, without encountering any singularities of the integrand, provided the vertical line has  $\text{Re}\{l\} \equiv L_2 > N(t)$ . The contribution of the semi-circle at infinity will vanish because of (2.5.5) and (A.30). Also these equations show that the region of convergence of (2.7.5) in  $z$  is much larger than the small Lehmann ellipse (2.4.11) within which (2.7.7) is valid. This region is independent of  $\text{Im}\{\theta\}$ , and in fact, because of (2.5.11), should include the whole  $z$  plane. The  $s$  singularities of  $A^{\mathcal{S}}(s, t)$  which prevent the convergence of (2.7.7) are present in  $P_l(-z_t)$ ,  $z_t > 1$ , for non-integer  $l$  through (A.13).

If we displace  $L_2$  to the left we shall encounter the  $l$ -plane singularities like (2.7.2), (2.7.4) which are responsible for the divergence of (2.6.2). Let us suppose for simplicity that we encounter just one pole at  $l = \alpha(t)$  of the form  $A_l(t) \sim \beta(t)(l - \alpha(t))^{-1}$ , and one branch point at  $l = \alpha_c(t)$  in  $\text{Re}\{l\} > -\frac{1}{2}$ , as shown in fig. 2.8. Then we obtain

$$\begin{aligned}
 A^{\mathcal{S}}(s, t) = & -\frac{16\pi}{2i} \int_{C_2} (2l + 1) A_l^{\mathcal{S}}(t) \frac{P_l(-z_t)}{\sin \pi l} dl \\
 & - 16\pi^2(2\alpha(t) + 1) \beta(t) \frac{P_{\alpha(t)}(-z_t)}{\sin \pi \alpha(t)} \\
 & - \frac{16\pi}{2i} \int^{\alpha_c(t)} (2l + 1) A_l^{\mathcal{S}}(t) \frac{P_l(-z_t)}{\sin \pi l} dl \quad (2.7.8)
 \end{aligned}$$

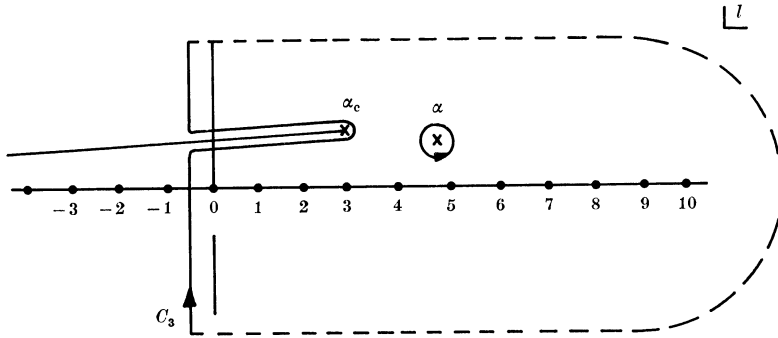


FIG. 2.8 The integration contour opened further to  $C_3$  along  $\text{Re}\{l\} = -\frac{1}{2}$ , exposing a pole at  $l = \alpha$  and making an excursion round the branch cut beginning at the branch point  $\alpha_c$ .

where the last term is the integration round the branch point shown in fig. 2.8,  $\Delta_l^{\mathcal{S}}(t)$  being the cut discontinuity. Equation (2.7.8) is known as the Sommerfeld–Watson representation.

Because of the asymptotic  $z$  behaviour of  $P_l(z)$  (see (A.25), (A.26)) it is evident that the first term, called the ‘background integral’,  $\sim s^{-\frac{1}{2}}$  as  $s \rightarrow \infty$  and so vanishes. Similarly, the pole term  $\sim s^{\alpha(t)}$  like (2.7.1), while the asymptotic behaviour of the cut depends on the form of its discontinuity at the branch point  $l \rightarrow \alpha_c(t)$ . If  $\Delta_l^{\mathcal{S}}(t)$  behaves like  $(l - \alpha_c(t))^{1+\beta(t)}$  then the asymptotic form is  $\sim s^{\alpha(t)} (\log s)^{\beta(t)}$ ; see (2.7.4).

In potential scattering, for well behaved potentials, there are only poles, no cuts, as Regge showed in his original papers on the subject (see chapter 3). In particle physics, we expect that there will be cuts as well, but we shall postpone detailed discussion of them until chapter 8, and for the time being concentrate on the poles.

### 2.8 Regge poles

The second term in (2.7.8) is called a ‘Regge pole’, i.e. a pole in the complex  $l$  plane. Its contribution to the scattering amplitude is

$$A^{\mathcal{S}R}(s, t) = -16\pi^2 (2\alpha(t) + 1) \beta(t) \frac{P_{\alpha(t)}(-z_t)}{\sin \pi\alpha(t)} \tag{2.8.1}$$

Because of (A.13) the  $s$  discontinuity takes the form

$$D_s^R(s, t) = 16\pi^2 (2\alpha(t) + 1) \beta(t) P_{\alpha(t)}(z_t), \quad z_t > 1$$

$$\sim s^{\alpha(t)} \tag{2.8.2}$$

$s \rightarrow \infty$

as expected from (2.7.1). In fact if (2.8.2) is substituted in (2.6.2) we find, from (A.22),

$$A_I^{\mathcal{S}}(t) = \frac{(2\alpha(t) + 1)\beta(t)}{(l - \alpha(t))(l + \alpha(t) + 1)} \xrightarrow{l \rightarrow \alpha(t)} \frac{\beta(t)}{l - \alpha(t)} \tag{2.8.3}$$

confirming that (2.8.1) does give rise to a pole in the  $l$  plane.

If  $\alpha(t)$  is a function of  $t$ , then, for a given fixed  $l$ ,  $A_I(t)$  will have a pole in  $t$  at the point  $t_r$  where  $\alpha(t_r) = l$ . We shall examine the properties of  $\alpha(t)$ ,  $\beta(t)$  in detail in section 3.2, and will find that usually  $\alpha(t)$  is a real analytic function of  $t$  with a branch point at the threshold  $t_T$ . Thus for real  $t > t_T$  we can separate it into its real and imaginary parts

$$\alpha(t) = \alpha_R(t) + i\alpha_I(t) \tag{2.8.4}$$

and define  $t_r$  to be the point where  $\alpha_R(t) = l$ . So expanding about this point gives

$$\alpha(t) = l + \alpha'_R(t_r)(t - t_r) + \dots + i\alpha_I(t_r) + i\alpha'_I(t_r)(t - t_r) + \dots \tag{2.8.5}$$

(where  $' \equiv d/dt$ ) and so for  $\alpha_R \approx l$

$$A_I^{\mathcal{S}}(t) \approx \frac{\beta(t_r)}{-\alpha'_R(t_r)(t - t_r) - i\alpha_I(t_r) - i\alpha'_I(t_r)(t - t_r)} \approx \frac{\beta(t_r)/\alpha'_R(t_r)}{t_r - t - i\alpha_I(t_r)/\alpha'_R(t_r)} \tag{2.8.6}$$

assuming  $\alpha'_I \ll \alpha'_R$ . This may be compared with the Breit-Wigner formula (2.2.15) from which we see that (2.8.6) corresponds to a  $t$ -channel resonance of mass  $M_r = \sqrt{t_r}$  and total width

$$\Gamma = \frac{\alpha_I(t_r)}{\alpha'_R(t_r)M_r} \tag{2.8.7}$$

Below threshold  $\alpha_I = 0$  and we have a bound state pole on the real  $t$  axis. This puts bound states and resonances on a very similar footing, both being Regge poles (fig. 2.9).

When such a Regge pole occurs for a physical integer value of  $l$  it will correspond to a physical particle or resonance. This is also evident from (2.8.1) in which we see that a pole in  $t$  will occur when  $\alpha(t)$  passes through an integer because of the vanishing of  $\sin \pi\alpha(t)$ . However, (2.8.1) is the signed amplitude, and to obtain the physical amplitude we must use (2.5.10) giving

$$A^R(s, t) = -16\pi^2(2\alpha(t) + 1)\beta(t) \frac{P_{\alpha(t)}(-z_t) + \mathcal{S}P_{\alpha(t)}(z_t)}{\sin \pi\alpha(t)} \tag{2.8.8}$$

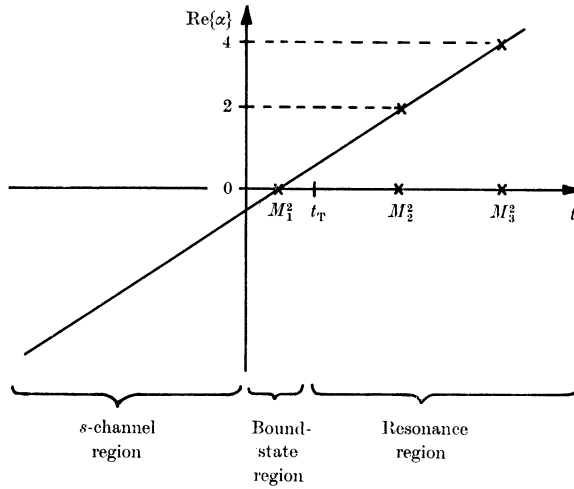


FIG. 2.9 A Regge trajectory of even signature. The trajectory has  $\text{Re}\{\alpha\} = 0$  for  $t < t_T$  (the threshold) giving a spin = 0 bound state of mass  $M_1$ , and then resonances of spin 2 mass  $M_2$ , and spin 4 mass  $M_3$ . For  $t < 0$  the trajectory contributes to the power behaviour of the crossed  $s$ -channel amplitude,  $\sim s^{\alpha(t)}$ .

which with (A.10) becomes

$$A^R(s, t) = -16\pi^2 (2\alpha(t) + 1) \beta(t) \left[ (1 + \mathcal{S} e^{-i\pi\alpha(t)}) \frac{P_{\alpha(t)}(-z_t)}{\sin \pi\alpha(t)} - \mathcal{S} \frac{2}{\pi} \sin \pi\alpha(t) Q_{\alpha(t)}(-z_t) \right] \quad (2.8.9)$$

But the last term is asymptotically negligible because of (A.27), and is usually omitted giving

$$A^R(s, t) = -16\pi^2 (2\alpha(t) + 1) \beta(t) (1 + \mathcal{S} e^{-i\pi\alpha(t)}) \frac{P_{\alpha(t)}(-z_t)}{\sin \pi\alpha(t)} \quad (2.8.10)$$

The factor  $(1 + \mathcal{S} e^{-i\pi\alpha})$  is called the ‘signature factor’, and it ensures that a trajectory of given signature  $\mathcal{S} = \pm 1$  contributes a pole in  $t$  to the scattering amplitude only when  $\alpha(t)$  passes through a right-signature integer (i.e. even/odd integer); see (2.5.4) *et seq.*

The Froissart bound (2.4.9) requires that  $\alpha(t) < 1$  for  $t < 0$ , but if trajectories rise through several integers for positive  $t$  we can expect to find families of particles which lie on the same trajectory, and whose spins are separated by 2 units of angular momentum. We shall find in chapter 5 that this is indeed the case, with  $\alpha(t)$  taking an approximately linear form

$$\alpha(t) = \alpha^0 + \alpha' t \quad (2.8.11)$$

as shown for example in fig. 2.9 and figs. 5.4–5.6. This provides one verification of the applicability of Regge’s ideas to particle physics.

Another simple test is to look at the crossed  $s$ -channel physical region  $s > s_T, t < 0$ . Here (2.8.10) gives, through (1.7.19) and (A.25),

$$A^R(s, t) \underset{s \rightarrow \infty}{\sim} s^{\alpha(t)} \tag{2.8.12}$$

where now  $t$  gives the momentum transfer. Hence we expect to find that at high energy the  $s$  dependence of the  $s$ -channel scattering amplitude is a simple power behaviour, the power being a function of the momentum transfer (remember  $\alpha(t)$  is real in this region). It should be an analytic continuation of the spins of the particles lying on the leading  $t$ -channel trajectory (see fig. 2.9 and fig. 6.6). Thus whereas  $\alpha(t)$  is observable only at discrete points for positive  $t$ , where  $\alpha(t) = \text{integer}$  and a particle occurs, it can be detected in the asymptotic  $s$  behaviour for all  $t < 0$ , at least in principle. In practice several trajectories may be exchanged in a given process making it hard to identify the different powers of  $s$  accurately, but it has proved possible to determine quite a lot of trajectories from the experimental data in this way—see section 6.8.

The power behaviour expected from the exchange of a Regge trajectory (sometimes called ‘Reggeon’) (2.8.12) may be contrasted with that from a fixed-spin (elementary) particle, (2.6.10), which corresponds to a Kronecker  $\delta$  in the  $l$  plane, (2.6.11). From (A.25) we see that (2.6.10) gives  $A(s, t) \sim s^\sigma$ , where  $\sigma$  is always integral, and independent of  $t$ . At first sight it is rather surprising that the exchange of many particles with high spins on a trajectory like fig. 2.9 should give rise to the power  $\alpha(t) < 1$  for  $t < 0$  (as required by the Froissart bound) when each particle individually would give  $s^i, i = 1, 2, 3, \dots$ . The reason for this is that, in a sense, the contributions of the different partial waves cancel; but remember the partial-wave series does not converge in the  $s$ -channel region. Thus suppose we have a linear trajectory like (2.8.11), with poles at

$$t = M_l^2 \equiv \frac{l - \alpha^0}{\alpha'}, \quad l = 0, 1, 2, \dots \quad (\alpha^0 < 0) \tag{2.8.13}$$

Then we can write the partial-wave series for these poles

$$\begin{aligned} A^{\mathcal{S}}(s, t) &= 16\pi \sum_l (2l + 1) \frac{\beta(M_l^2)}{\alpha'(M_l^2 - t)} P_l(z_t) \\ &= -\frac{16\pi}{2i} \int_{C_1} (2l + 1) \frac{\beta(t)}{l - \alpha(t)} \frac{P_l(-z_t)}{\sin \pi l} dl \end{aligned} \tag{2.8.14}$$



and when we apply the Sommerfeld–Watson transform (2.7.8) we find of course that  $A^{\mathcal{S}}(s, t) \sim s^{\alpha(t)}$ .

The hypothesis of maximal analyticity of the second kind implies that all the subtractions needed in dispersion relations such as (1.10.7) are due to singularities in the angular-momentum plane like (2.7.2) and (2.7.4). If we allowed arbitrary subtractions, as in (1.10.10), the function  $F_{n-1}(s, t)$  (a polynomial of degree  $n-1$  in  $s$ ) would contribute to all the (integer) partial waves  $l = 0, 1, 2, \dots, n-1$  in the  $t$  channel, giving Kronecker  $\delta$  terms in the  $l$  plane,  $\delta_{l0}, \delta_{l1}, \dots, \delta_{ln-1}$ , rather than singularities. But such terms are precluded by our analyticity postulate. The Froissart bound implies that the degree of  $F_{n-1}(s, t)$  can be at most 1, so the higher partial waves are certainly obtainable from  $D_s^{\mathcal{S}}(s, t)$ ; but the analyticity postulate also requires that the lowest partial waves should be obtained from the higher by analytic continuation, so they are given by  $D_s^{\mathcal{S}}(s, t)$  too, and  $F$  is not arbitrary.

This closes a most important gap in the determination of the scattering amplitude by the unitarity equations. For we have seen in chapter 1 (especially section 1.10) that given all the particle poles (masses and couplings) one can, in principle, determine all the other singularities from the unitarity equations, and thence find the scattering amplitudes by using dispersion relations (apart from the subtractions). But there seemed to be no limitation on the number of particles which could occur. However, it is unlikely that one needs to put in all the particle poles *a priori*, since the composite particles which are generated by the forces should emerge as consequences of unitarity, and will lie on trajectories. For example, if one regards the deuteron as a neutron–proton bound state it should be possible to deduce its properties (mass and coupling) from a knowledge of the strong interaction forces, and it would be inconsistent to insert arbitrary values for these quantities.

Now maximal analyticity of the second kind tells us that if one knows  $D_s^{\mathcal{S}}(s, t)$  one can work back, via the Froissart–Gribov projection, and determine the nature of all the poles, because they are all Regge poles. This requires a very high degree of self-consistency in strong-interaction theory. For if we were to try and invent a new particle, and insert it into the unitarity equations, it would generate further singularities, and hence further contributions to the asymptotic behaviour of the scattering amplitudes, and hence further Regge poles which would themselves have to be included in the unitarity equations – and so on.

Clearly if our postulates are correct the actual (perhaps infinite) number of different types of particles in the universe must be self-consistent, i.e. must reproduce itself, and no other particles, under the combined processes of unitarization and analytic continuation in  $l$ . But whether it is the unique set with this property, so that the self-consistency requirement determines the theory completely, is not clear. The proposal that all the strongly interacting particles are self generating in this way is called the 'bootstrap hypothesis' (see Chew 1962) and we shall examine it further below. Intuitively, it seems clear that if all the hadrons are to be composites of each other, and all the forces are due to the exchange of particles, then some form of self-consistency is necessary, and by invoking Regge theory it is possible to give a more rigorous formulation of this idea. Since this proposal eliminates elementary particles, and puts all the observed particles on an equal footing as composite Reggeons, it is sometimes referred to as 'nuclear democracy' (Chew 1965).

Alternatively, it may be that there are some basic elementary particles, for example quarks (see chapter 5), which do not lie on Regge trajectories, and whose properties one needs to know before one can predict the particle spectrum. If so, Regge theory will not be sufficient by itself to tell us everything about strong-interaction physics, but it will still provide important consistency constraints on scattering amplitudes. We shall return to these more philosophical problems in chapter 11.

### 2.9 The Mandelstam–Sommerfeld–Watson transform\*

In (2.7.8) we chose the contour for the background integral,  $C_3$ , along  $\text{Re}\{l\} = -\frac{1}{2}$  because (see (A.25), (A.26)) this gives the most convergent behaviour of  $P_l(z)$  ( $\sim z^{-\frac{1}{2}}$  for  $\text{Re}\{l\} = -\frac{1}{2}$ ). However, this line is not a natural boundary of analytic continuation, and Mandelstam (1962) has shown how it may be crossed.

We begin by rewriting (2.7.7) as

$$A^{\mathcal{S}}(s, t) = 16\pi \sum_{l=0}^{\infty} \left\{ (2l+1) A_l(t) P_l(z_t) + \frac{1}{\pi} (-1)^{l-1} (2l) A_{l-\frac{1}{2}}^{\mathcal{S}}(t) Q_{l-\frac{1}{2}}(z_t) \right\} - 16\pi \sum_{l=1}^{\infty} \frac{1}{\pi} (-1)^{l-1} (2l) A_{l-\frac{1}{2}}^{\mathcal{S}}(t) Q_{l-\frac{1}{2}}(z_t) \quad (2.9.1)$$

We then make a Sommerfeld–Watson transform of the two terms in

\* This section may be omitted at first reading.

brackets { } in (2.9.1), the first giving (2.7.5) and the second involving  $Q_l(-z_t)(\cos \pi l)^{-1}$  which has the required poles at half-integer values of  $l$ . Then using (A.18) these two integrals can be combined giving, when we open up the contour as in (2.7.6),

$$\begin{aligned}
 A^{\mathcal{S}}(s, t) &= \frac{16}{2i} \int_{-\frac{1}{2}+\epsilon-i\infty}^{-\frac{1}{2}+\epsilon+i\infty} (2l+1) A_l^{\mathcal{S}}(t) \frac{Q_{-l-1}(z_t)}{\cos \pi l} dl \\
 &\quad + 16\pi(2\alpha(t)+1)\beta(t) \frac{Q_{-\alpha(t)-1}(-z_t)}{\cos \pi \alpha(t)} \\
 &\quad + \frac{16}{2i} \int^{\alpha(t)}_{-\infty} (2l+1) A_l^{\mathcal{S}}(t) \frac{Q_{-l-1}(-z_t)}{\cos \pi l} dl \\
 &\quad - 16\pi \sum_{l=1}^{\infty} \frac{1}{\pi} (-1)^{l-1} (2l) A_{l-\frac{1}{2}}^{\mathcal{S}}(t) Q_{l-\frac{1}{2}}(z_t) \quad (2.9.2)
 \end{aligned}$$

The contour of the background integral has been put at  $\frac{1}{2} + \epsilon$  ( $\epsilon > 0$ ) to avoid the pole of  $(\cos \pi l)^{-1}$  at  $l = -\frac{1}{2}$  (fig. 2.10). If we now displace this contour to  $\text{Re}\{l\} = -l$  we pick up contributions from the poles at  $l \equiv l'$  (say)  $= -\frac{1}{2}, -\frac{3}{2}, \dots, -L'$ , where  $-L'$  is the first half-integer above  $-L$ , giving

$$\begin{aligned}
 A^{\mathcal{S}}(s, t) &= \frac{16}{2i} \int_{-L-i\infty}^{-L+i\infty} (2l+1) A_l^{\mathcal{S}}(t) \frac{Q_{-l-1}(-z_t)}{\cos \pi l} dl + \text{poles} + \text{cuts} \\
 &\quad - 16\pi \sum_{l'=-L'}^{-\frac{1}{2}} (2l'+1) A_{l'}^{\mathcal{S}}(t) Q_{-l'-1}(-z_t) \frac{(-1)^{l'-\frac{1}{2}}}{\pi} \\
 &\quad - 16\pi \sum_{l=1}^{\infty} \frac{(-1)^{l-1}}{\pi} (2l) A_{l-\frac{1}{2}}^{\mathcal{S}}(t) Q_{l-\frac{1}{2}}(z_t) \quad (2.9.3)
 \end{aligned}$$

If we now replace the summation index  $l'$  in the second line by  $l = -l' - \frac{1}{2}$ , this line becomes

$$16\pi \sum_{l=0}^{L'-\frac{1}{2}} \frac{(-1)^{-l-1}}{\pi} (-2l) A_{l-\frac{1}{2}}^{\mathcal{S}}(t) Q_{l-\frac{1}{2}}(-z_t) \quad (2.9.4)$$

which will cancel with the first  $L' - \frac{1}{2}$  terms of the last summation in (2.9.3) provided

$$A_{l-\frac{1}{2}}^{\mathcal{S}}(t) = A_{-l-\frac{1}{2}}^{\mathcal{S}}(t) \quad \text{for } l = \text{integer} \quad (2.9.5)$$

This symmetry of partial-wave amplitudes about  $l = -\frac{1}{2}$ , the so-called ‘Mandelstam symmetry’, follows from the Froissart–Gribov projection (2.6.2) and the corresponding symmetry (A.19) of  $Q_l(z)$  (except that of course the projection does not converge without subtractions), and as we shall see in the next chapter it is true in

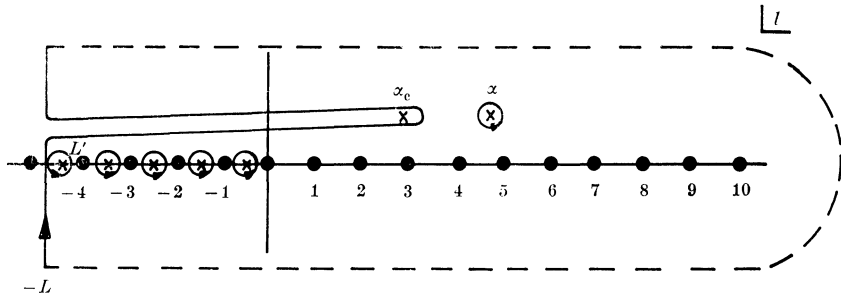


Fig. 2.10 The integration contour in (2.9.2) with the same singularities as fig. 2.8, but we also pick up extra poles at the negative half-integers.

potential scattering, so it seems reasonable to suppose that it will also hold in strong interactions. If so we end up with

$$\begin{aligned}
 A^{\mathcal{S}}(s, t) = & \frac{16}{2i} \int_{-L-i\infty}^{-L+i\infty} (2l+1) A_l^{\mathcal{S}}(t) \frac{Q_{-l-1}(-z_t)}{\cos \pi l} dl + \text{poles} + \text{cuts} \\
 & - 16 \sum_{l=L+\frac{1}{2}}^{\infty} (-1)^{l-1} (2l) A_{l-\frac{1}{2}}^{\mathcal{S}}(t) Q_{l-\frac{1}{2}}(z_t) \quad (2.9.6)
 \end{aligned}$$

Since from (A.27)  $Q_l(z) \sim z^{-l-1}$ , the Regge pole and cut terms (given explicitly in (2.9.2)) still have the asymptotic behaviour  $\sim s^{\alpha(t)}$ , but the first and last terms of (2.9.6)  $\sim s^{-L}$  where  $L$  can be made as large as we like. Of course in displacing the contour in this way we can expect to expose more poles and cuts, and the magnitude of the background integral at fixed  $z$  may increase.

The actual pole in the Regge term in (2.9.2) has been absorbed into  $Q_{-\alpha-1}$ , which has poles for  $\alpha =$  a non-negative integer (see (A.32)). The apparent poles from  $(\cos \pi \alpha)^{-1}$ , at positive half-integer values of  $\alpha$ , cancel with the zeros of  $Q_{-\alpha-1}$  which contains  $(\Gamma(-\alpha + \frac{1}{2}))^{-1}$  (see (A.8)) while the symmetry (2.9.5) ensures that the residues of these poles vanish for negative half-integers.

**2.10 The Mellin transform\***

Frequently we shall be concerned only with the leading asymptotic  $s$  behaviour of the scattering amplitude, in which case many of our equations can be greatly simplified by including only the asymptotic behaviour of the Legendre functions, (A.25), (A.27), and making the replacement  $z_t \rightarrow s$  for  $s \rightarrow \infty$ .

\* This section may be omitted at first reading.

Thus instead of the  $t$ -channel partial-wave series (2.5.6) we write the power series expansion

$$A^{\mathcal{S}}(s, t) = \sum_{n=0}^{\infty} a_n(t) s^n \quad (2.10.1)$$

The dispersion relation (2.5.8) may be expanded in the form

$$\begin{aligned} A^{\mathcal{S}}(s, t) &= \frac{1}{\pi} \int_{s_T}^{\infty} \frac{D_s^{\mathcal{S}}(s', t)}{s' - s} ds' \\ &= \frac{1}{\pi} \int_{s_T}^{\infty} D_s^{\mathcal{S}}(s', t) \frac{1}{s'} \left[ 1 + \frac{s}{s'} + \left( \frac{s}{s'} \right)^2 + \dots \right] ds' \end{aligned} \quad (2.10.2)$$

and on comparing with (2.10.1) for each power of  $s$  we find

$$a_n(t) = \frac{1}{\pi} \int_{s_T}^{\infty} D_s^{\mathcal{S}}(s', t) s'^{-(n+1)} ds' \quad (2.10.3)$$

which corresponds to taking the leading  $s$  term of the Legendre function in the Froissart–Gribov projection (2.5.3). However, the position of the threshold is irrelevant as far as the leading behaviour is concerned, and so it will not make much difference if we write instead of (2.10.3)

$$a_n(t) = \frac{1}{\pi} \int_0^{\infty} D_s^{\mathcal{S}}(s', t) s'^{-(n+1)} ds' \quad (2.10.4)$$

This is the Mellin transform of  $D_s^{\mathcal{S}}(s', t)$  (see Titchmarsh (1937) p. 7), and its inverse is

$$D_s^{\mathcal{S}}(s, t) = \frac{1}{2i} \int_{-i\infty+\gamma}^{i\infty+\gamma} a_n(t) s^n dn \quad (2.10.5)$$

where the contour of integration is along a line parallel to the imaginary axis to the right of all the singularities in  $n$  of  $a_n(t)$ .

Now if we take the leading power of the Legendre function in the Sommerfeld–Watson transform (2.7.5) we get

$$A^{\mathcal{S}}(s, t) = -\frac{16\pi}{2i} \int_{C_1} (2l+1) A_l^{\mathcal{S}}(t) \frac{(-s)^l}{\sin \pi l} dl \quad (2.10.6)$$

which agrees with (2.10.5) if we remember that

$$\text{Disc}_s \{(-s)^l\} = -s^l \sin \pi l, \quad s > 0,$$

and if we incorporate the factor  $16\pi(2l+1)$  into  $a_n(t)$ . The contour  $C_1$  in (2.10.6) can be expanded to that in (2.10.5), but if  $D_s^{\mathcal{S}}(s, t) \sim s^{\alpha(t)}$  then  $a_n(t)$  will obtain a pole at  $n = \alpha(t)$  from (2.10.3) (see (2.7.2)), whose contribution will have to be added to (2.10.5) similar to (2.7.8). Hence Regge poles in the  $l$  plane give rise to poles in the  $n$  plane. However,

since the Legendre function can be expanded as a power series in  $z_t$ , of which (A.25) is only the first term, a given Regge pole will produce a series of poles in the  $n$  plane at  $n = \alpha(t) - m$ ,  $m = 0, 1, 2, \dots$ ; and vice versa. But as long as we are only concerned with the leading behaviour this many-to-one correspondence between poles in the  $l$  and  $n$  planes will not matter.

The dispersion properties are somewhat different in that (2.10.6) is cut for  $0 \leq s \leq \infty$  while the pole in (2.7.8) is cut for  $z_t > 1$  (see (A.13)), i.e.  $-4q_t^2 \leq s \leq \infty$  for equal-mass kinematics, from (1.7.22). Of course neither of these is correct because the  $s$  cuts of the amplitude should start at the threshold  $s = s_T$ . So there must be a cancellation between the discontinuities of the pole terms and the background integral in the regions  $0 \leq s \leq s_T$  and  $-4q_t^2 \leq s \leq s_T$ , respectively. Also we shall find in chapter 6 that the replacement of  $z_t$  by  $s$  is not always trivial with unequal-mass kinematics. But provided these points are borne in mind it is frequently convenient to use (2.10.4) and (2.10.5) instead of the more exact expressions.